

PROGRESS IN THE DESIGN OF BEAM OPTICS FOR FCC-ee COLLIDER RING*

K. Oide[†], K. Ohmi, KEK, Tsukuba, Japan
 A. Bogomyagkov, E. Levichev, D. Shatilov, BINP SB RAS, Novosibirsk, Russia
 M. Benedikt, H. Burkhardt, B. Holzer, A. Milanese,
 J. Wenninger, F. Zimmermann, CERN, Geneva, Switzerland
 A. Blondel, M. Koratzinos, DPNC/Geneva University, Geneva, Switzerland
 M. Boscolo, INFN/LNF, Frascati, Italy

Abstract

The FCC-ee is a double-ring e^+e^- collider to be installed in a common tunnel of ~ 100 km circumference, as a potential first step before the FCC-hh hadron collider. The beam energy covers at least from the Z-pole (45.6 GeV) to $t\bar{t}$ (175 GeV) threshold. The design restricts the total synchrotron radiation (SR) power at 100 MW, thus the stored current per beam varies from 1.4 A at Z to 6.4 mA at $t\bar{t}$.

An update has been performed on the “baseline” beam optics [1] for the FCC-ee double-ring e^+e^- collider. The major changes are: (a) mitigation of the coherent beam-beam instability at Z by squeezing β_x^* down to 15 cm and changing the arc phase advance to $60^\circ/60^\circ$, (b) application of the twin aperture quadrupole scheme [2] to save the power consumption of quadrupole magnets, (c) fit to a modified layout of the FCC-hh collider.

The main characteristics of the optics design have been preserved: 45 to 175 GeV beam energy, ~ 100 km circumference with two interaction points (IPs) per ring, horizontal crossing angle of 30 mrad at the IP, and the crab-waist scheme with local chromaticity correction system. A so-called “tapering” of the magnets is applied, which scales all fields of magnets with the local beam energy determined by the SR. An asymmetric layout near the interaction region suppresses the critical energy of SR incoming to the detector at the IP below 100 keV. Sufficient transverse/longitudinal dynamic apertures (DAs) have been obtained to assure adequate beam lifetime with beamstrahlung and top-up injection.

MITIGATION OF COHERENT BEAM-BEAM INSTABILITY

A coherent beam-beam instability in the x - z plane was first found by K. Ohmi by a strong-strong beam-beam simulation at the beam energy 45.6 GeV [3]. Afterwards the same phenomenon was confirmed by D. Shatilov in a completely independent simulation based on a turn-by-turn alternating quasi-strong-strong model. Both simulations agree with each other in the instability threshold, the magnitude of the beam blowup above threshold, and the dependences of the instability on various beam parameters. The effect of this

Table 1: The Parameters of FCC-ee with the Updated Optics at Beam Energies 45.6 GeV (Z) and 175 GeV ($t\bar{t}$).

Circumference [km]	97.750	
Arc quadrupole scheme	twin aperture	
Bend. radius of arc dipole [km]	10.747	
Number of IPs / ring	2	
Crossing angle at IP [mrad]	30	
Solenoid field at IP [T]	± 2	
ℓ^* [m]	2.2	
Local chrom. correction	y-plane with crab-sext. effect	
RF frequency [MHz]	400	
Total SR power [MW]	100	
Beam energy [GeV]	45.6	175
SR energy loss/turn [GeV]	0.0360	7.80
Long. damping time [ms]	414	7.49
Polarization time [s]	9.2×10^5	1080
Current/beam [mA]	1390	6.4
Bunches/ring	70760	62
Particles/bunch [10^{10}]	4.0	21.1
Arc cell	$60^\circ/60^\circ$	$90^\circ/90^\circ$
Mom. compaction α_p [10^{-6}]	14.79	7.31
Horizontal tune ν_x	269.14	389.08
Vertical tune ν_y	267.22	389.18
Arc sext. families	208	292
Horizontal emittance ε_x [nm]	0.267	1.34
$\varepsilon_y/\varepsilon_x$ at collision [%]	0.38	0.2
β_x^* [m]	0.15	1
β_y^* [mm]	1	2
Energy spread by SR [%]	0.038	0.144
RF Voltage [MV]	255	9500
Bunch length by SR [mm]	2.1	2.4
Synchrotron tune ν_z	-0.0413	-0.0684
RF bucket height [%]	3.8	10.3
Luminosity/IP [$10^{34}/\text{cm}^2\text{s}$]	121	1.32

instability is significant, e.g. it can reduce the luminosity to $\sim 30\%$ of the original design value at Z.

A semi-analytical scaling law for the threshold bunch intensity is [4]

$$N_{\text{th}} \propto \frac{\alpha_p \sigma_\delta \sigma_z}{\beta_x^*}, \quad (1)$$

where α_p , σ_δ , σ_z , and β_x^* denote the momentum compaction factor, the energy spread, the bunch length, and the horizontal β -function at the interaction point (IP), respectively. According to Eq. (1), a smaller β_x^* and a larger α_p help suppress the instability. Thus we have sought a new optics to mitigate the instability through reducing β_x^* from 50 cm to 15 cm and increasing α_p by a factor of 2 with a $60^\circ/60^\circ$ (instead of $90^\circ/90^\circ$) FODO cell in the arc. The other parameters have been re-optimized to maximize the luminosity. The results are summarized in Table. 1. Note

* Work supported by the European Commission under Capacities 7th Framework Programme project EuCARD-2, grant agreement 312453, and under the Horizon 2020 Programme project CREMLIN, grant agreement 654166.

[†] Katsunobu.Oide@kek.jp

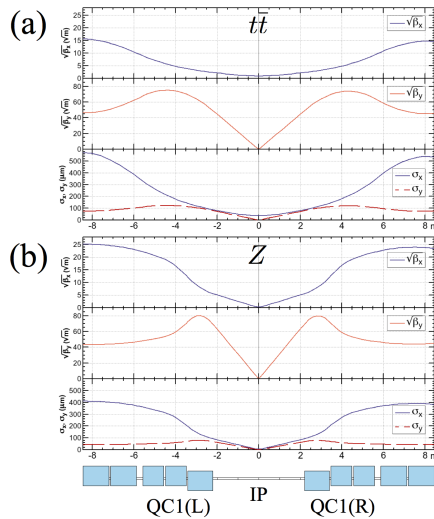


Figure 1: The β -functions and beam sizes around the IP at (a) $\bar{t}\bar{t}$ and (b) Z . The beam sizes assume the equilibrium emittances listed in Table 1. The final quadrupoles QC1(L/R) are longitudinally split into three slices.

that the beamstrahlung enlarges both σ_δ and σ_z in Eq. (1) and, therefore, relaxes the threshold. The bunch intensity in Table 1 is chosen below the threshold assuming values for σ_δ and σ_z due to the synchrotron radiation (SR) only. Thus, in collision, we may gradually increase the bunch intensity further by topping up, after the beams have reached an equilibrium with beamstrahlung, and obtain a luminosity higher than quoted.

Smaller β_x^* at the IP

To reduce β_x^* at the Z from the original value, 50 cm, to 15 cm, we split the final vertical focusing quadrupole QC1, which is placed at $\ell^* = 2.2$ m from the IP, into three pieces. While at higher energies, all three pieces provide vertical focusing, at the Z only the first piece remains vertically focusing while the remaining two focus horizontally. The field strengths are limited to the same value (100 T/m) at all beam energies. By this triple splitting, the center of focusing for each plane moves closer towards the IP at the Z , which reduces the chromaticity for the smaller β^* . Comparing Figure 1 (a) and (b) we see that the beam sizes at the Z through this region are still smaller than those at $\bar{t}\bar{t}$. The peak value of β_y is almost unchanged even though β_y^* is reduced by 1/2. The peak of β_x is only 60% higher, while β_x^* becomes 1/6 of the value at higher energy.

60°/60° Arc Cell at Z

The previous design of the arc optics was based on a 90°/90° FODO cell, which efficiently accommodated non-interleaved sextupole pairs. Since at the Z we need a higher momentum compaction factor to mitigate the beam-beam instability, as discussed above, we here change the phase advances to 60°/60°. At higher energies we keep the original 90°/90° lattice. The cell length is fixed at 55.89 m. An issue is that, in order to maintain the non-interleaved sextupole scheme at the Z , we have to insert sextupoles at different

locations from the case of 90°/90°, while some of them may be common. As the sextupoles for 60°/60° are only needed at the Z , these can be thinner. Thus we split the sextupoles used for 90°/90° into short and long pieces, 0.7 m and 1.4 m long, respectively, as shown in Fig. 2. Only the short one is used at the Z , and may get a short new counterpart. By doing so, we minimize the overall spaces allocated to sextupoles and improve the dipole packing factor in the arc.

The 60°/60° arc also increases the horizontal emittance by a factor of 3. However, the horizontal emittance does not affect the luminosity for collisions with a large Piwinski angle and the crab-waist scheme. For a lattice with even smaller phase advances per cell, the still higher horizontal emittance would result in a vertical emittance larger than our design goal 1 pm at the Z , assuming 0.2% emittance ratio. Another way to increase the momentum compaction is a making use of a combined function dipole as discussed in Ref. [1]. However, as the associated energy spread becomes too large to ensure the polarization for a pilot bunch, esp. at W^\pm , we exclude the combined function.

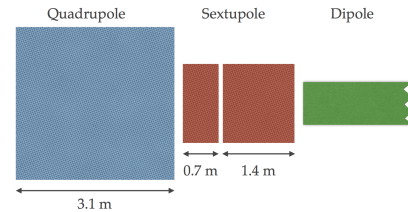


Figure 2: The sextupole in the arc is split in short/long ones. Only the short one is used for the 60°/60° cell for Z . The long piece, depending on location, may be filled with a dipole to improve the packing factor.

TWIN APERTURE QUADRUPOLE

This update of the optics employs the “twin aperture quadrupole” scheme [2] for the arc lattice. Figure 3 illustrates a possible cross section of such a quadrupole. This scheme encloses the current of the magnet coil completely with iron to maximize the power efficiency. The power for the twin quadrupoles is estimated as 22 MW at $\bar{t}\bar{t}$ for the total of two rings. A regular single aperture quadrupole would double the power consumption. The dipoles are also of twin aperture type, and consume about 17 MW at the $\bar{t}\bar{t}$ for the two rings together.

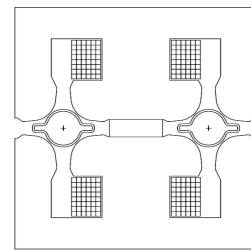


Figure 3: A possible cross section of the “twin aperture” quadrupole magnet. Currently we assume 30 cm for the beam separation and 35 mm radius for the inner radius of the beam pipe. In this scheme, a quadrupole has opposite signs of focusing for the two beams.

A drawback of this scheme is that the packing factor is slightly reduced, since both the horizontal and vertical quadrupoles need to have the same length, which would not be necessary from the point of view of the optics. Thus, while the twin-aperture quadrupoles save power for the quadrupoles, they increase the SR power. The total loss is more significant at lower beam energies. Another drawback is a complication in the lattice design, especially for the dispersion suppressors.

FITTING TO FCC-hh LAYOUT

The FCC-ee collider must keep the same footprint as the associated hadron collider, FCC-hh, except for a few kilometers around the IP. Recently the tunnel for FCC-hh has been modified to better adapt to the geological conditions around Geneva [5]. The resulting footprint shortens the straight sections J and D (see Fig. 4), which are used for the RF sections of FCC-ee, from 4.2 km to 2.8 km each. Also the locations of intermediate straight sections B, D, H, J are slightly shifted. Thus FCC-ee followed the change, but its effect on the performance was minimal.

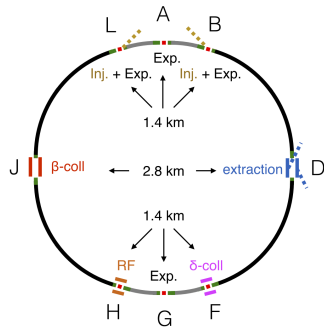


Figure 4: A new layout of the FCC-hh collider footprint. The detectors and RF for FCC-ee are placed at straight sections A/G and D/J, respectively. Other straight sections are used for injection, extraction, collimation, diagnostics, etc.

DYNAMIC APERTURE

Dynamic aperture (DA) has been estimated in the same way as described in Ref. [1], by a full-symplectic 6D tracking code SAD [6]. A number of effects are taken into account including synchrotron motion, synchrotron radiation damping in dipoles and quadrupoles, crab-waist, nonlinear Maxwellian fringes for all magnets, and kinematical terms. Solenoids around the IP are not included for the time being to ensure a compatibility with MAD-X, but their effect on the dynamic aperture is negligible, as long as a local compensation is applied [1].

The DA has been optimized by searching optimum sextupole settings through particle tracking with the downhill simplex method scripted in SAD. Figure 5 shows a result of such an optimization. The resulting DA matches the requirements for both beam-beam and injection, at least without any errors and misalignments.

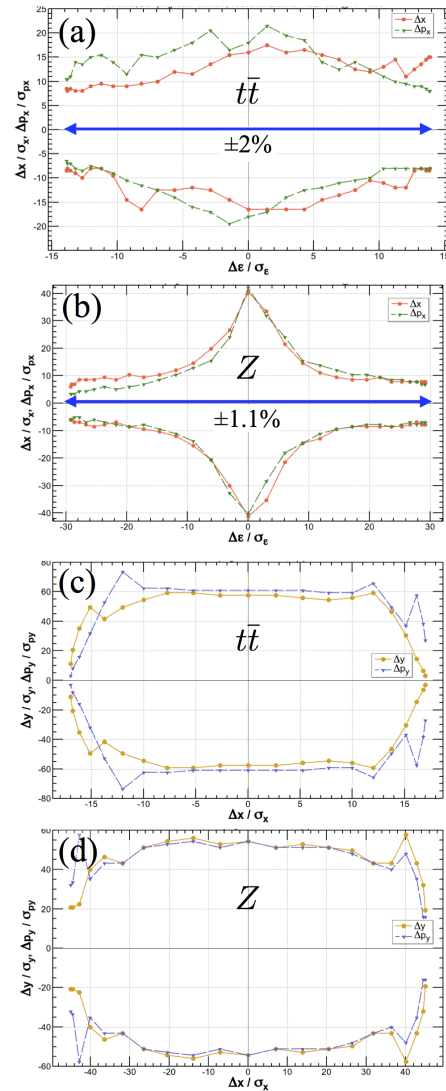


Figure 5: The dynamic apertures after an optimization of sextupoles via particle tracking; (a, c): $\beta_{x,y}^* = (1 \text{ m}, 2 \text{ mm})$, 50 turns at $t\bar{t}$, and (b, d): $\beta_{x,y}^* = (15 \text{ cm}, 1 \text{ mm})$, 2,550 turns at the Z; (a, b): z - x plane; (c, d): x - y plane.

The resulting dynamical momentum acceptances are $\pm 2\%$ and $\pm 1.1\%$, which correspond to $\pm 10\sigma$ and $\pm 13\sigma$ of the estimated energy spreads including the beamstrahlung, 0.19% and 0.083%, at $t\bar{t}$ and Z, respectively. The transverse aperture near on-energy is sufficiently large for on-energy top-up injection.

ACKNOWLEDGEMENT

The authors thank D. Schulte and A. S. Langner for providing the new layout of FCC-hh. They also thank S. Aumon, E. Belli, B. Harer, P. Janot, R. Kersevan, D. El-Khechen, A. Novokhatski, S. Ogur, J. Seeman, S. Sinyatkin, H. Sugimoto, M. Sullivan, T. Tydecks, D. Zhou for useful discussions and suggestions.

REFERENCES

[1] K. Oide et al., “Design of Beam Optics for the Future Circular Collider e^+e^- Collider Rings”, Phys. Rev. Accel. Beams, vol.

- 19, p. 111005, 2016.
- [2] A. Milanese, “Efficient Twin Aperture Magnets for the Future Circular e^+e^- Collider”, Phys. Rev. Accel. Beams, vol. 19, p. 112401, 2016.
 - [3] K. Ohmi, presentation at FCC Week 2016, Rome, Italy, 2016.
 - [4] K. Ohmi and N. Kuroo, “Coherent Beam-Beam Instability in Collision with a Large Crossing Angle”, presented at IPAC’17, Copenhagen, Denmark, May 2017, paper THPAB021, this conference.
 - [5] D. Schulte and A. S. Langner, private communications.
 - [6] <http://acc-physics.kek.jp/SAD/index.html>,
<https://github.com/KatsOide/SAD>